Neutral Density Enhancements due to Space Weather Effects

F. Herrero[a], A. Nicholas[b], D.Perez[c], P. Vu[d], E. Long[d], J. Ielmini[d]

a) Space Systems Research Corporation, Alexandria, VA 22314,
b) U. S. Naval Research Laboratory, Washington DC 20375,
c) DP Consultants, Melbourne, FL 32904,
d) OrboticSystems, Thousand Oaks, CA 91360

ABSTRACT

Earth's thermosphere and ionosphere are in thermal equilibrium up to about 500km altitude[1]. Therefore, satellites in this region are impacted by neutrals and ions with fluxes that are readily derivable from their Maxwellian velocity distributions - these distributions specified by the state parameters sought, namely, the bulk velocity vectors (neutral wind and ion-drift), with the temperatures and densities. Therefore, measurements of the energy and angle distributions of the fluxes with a suitable spectrometer on a satellite can be compared in least squares with the derived distributions to obtain the neutral wind $\vec{W}$ and ion-drift $\vec{V}_I$ together with neutral and ion temperatures and densities. These parameters and their gradients are the agents of neutral and ion transport that produce density enhancements in the thermosphere, and their knowledge are the required input data to predict energy enhancements in the thermosphere. Their measurement requires precision on particle energies and angles; these are new requirements that present challenges in neutral wind measurements that use electron impact ion sources for neutral-to-ion conversion together with ion energy analyzers for precise energy measurements. These challenges are addressed by the Wind-Ion-Neutral-Density (WIND) suite of spectrometers.

The drag force $F_D = 1/2\rho V^2 C_D A_r$ that air molecules exert on satellites slows satellites down reducing their altitudes and speeding them up. The primary factor in F_D is the density ρ that consists mainly of atomic oxygen O and molecular nitrogen N_2 at altitudes of interest, 200 to 500km. The 2nd factor V is the mean velocity of the impacting particles and is best represented by the ram velocity vector $\vec{V}_{Ram} = \vec{V}_{Sat} + \vec{W}$. Considering only circular orbits, V_{Sat} increases with decreasing altitude, being about 7.67km/s at 400km and 7.73km/s at 300km to increase drag by about 1.6% solely by the V_{Sat} change[1]. The wind W also affects V_{Ram} though it seldom exceeds 200m/s except in the polar regions where the zonal component of W is known to be as high as 1km/s [2]; this would impact the satellite orbit by a calculable amount if $\vec{W}$ were known. However, the effect, though finite, is diminished on likely polar orbits because $\vec{V}_{Sat} \perp W_{zonal}$, changing the drag by roughly 1.5%[2]. On the other hand a satellite in equatorial orbit would experience a $\pm 5\%$ change in drag force with a $\pm$200m/s equatorial zonal wind change. Thus, neutral wind effects, if large over some distance and time, could alter a satellite's orbit sufficiently to bring it close to other satellites as the effect accumulates over multiple passes.

The density ρ is the dominant factor in satellite orbits and its prediction is paramount for satellite operations aimed at reducing the possibility of satellite collisions[3]. However, density is only one of 10 parameters that interact closely to determine the state of the thermosphere; the other 9 required to obtain magnitude and location of any density enhancement. The 10 parameters reflect the importance of mass, momentum, and energy transport in the physics of the thermosphere and they are: the bulk velocity vector with three components, e.g, zonal, latitudinal, and vertical, that we write as u, v, w for the neutrals and $u_I, v_{,I} w_I$ for the ions; those together with the neutral temperature T and density ρ, and ion temperature T_I and density ρ_I. The 10 parameters $(u, v, w, T, \rho), (u_I, v_{,I} w_I, T_I, \rho_I)$ are the computer inputs that start the prediction process in computers in NOAA's Space Weather Prediction Program to account for the intricate couplings between neutrals and ions of the thermosphere in the presence of Earth's geomagnetic field. It is the function of WIND to provide these 10 parameters with a time cadence as fast as 1 second to telemeter to the ground as devised by mission requirements.

[1] In kinetic energy estimates for our spectrometer design we assume $V_{Ram} \simeq 8000$m/s.

[2] This may be larger if the satellite's drag force factors C_D and A_r are larger in the direction $\perp$ to $\vec{V}_{Ram}$.

[3] This paper does not address the problems of navigation and attitude control that would require onboard propulsion of adequate power and satellite mass and moments of inertia

A network of WIND instruments in orbit may thus provide NOAA's Space Weather Prediction Center (SWPC) with real-time data on the 10 parameters to enable rapid predictions of neutral density enhancements and unusually large neutral winds. Those data, taken at multiple points in the thermosphere and assimilated into SWPCs computer models ultimately lead to collision avoidance maneuvers to reduce risk of satellite collisions in an increasingly congested space environment. Further, these data can benefit other atmospheric models, both government and commercial in addition to being at the forefront of the science of thermosphere dynamics.

WIND uses a next-generation wind spectrometer WS described in this paper. WS is designed to measure both neutral and ion energy-angle distributions with the same unprecedented precision demonstrated previously for ions in the Wind-Ion-Neutral-Composition-Suite WINCS [4, 5]. In that sense, WIND builds upon the WINCS heritage for its energy analyzer[6] but goes further to solve the problem with the WINCS ion source that distorted the energy and angular distributions of the ionized neutrals to render them undetectable[7]. Therefore, the WIND suite has a new ion source, the Aperture Ion Source (AIS) designed to preserve enough of the energy/angle information of the neutrals while yielding sufficient signal to yield useful wind data.

The Wind-Ion-Neutral-Composition-Suite (WINCS) was developed to obtain neutral wind $\vec{W}$ and ion-drift $\vec{V}_I$ vectors, temperatures and densities plus neutral/ion composition. A joint effort between NASA's Goddard Space Flight Center (GSFC) and the U.S. Naval Research Laboratory (NRL), WINCS has flown on DoD's STP-Sat3, STP-H4, and NASA's GPIM [4, 5, 6].

WIND inherits from WINCS its energy analyzer - the Small-Deflection-Energy-Analyzer (SDEA) that scans the kinetic energy of ionized neutrals to measure their energy distributions simultaneously at multiple angles to generate the desired energy and angle distributions. WINCS used two identical spectrometers each with two SDEA chambers - one for incident neutrals (which are ionized for detection) and one for incident ions. One spectrometer is oriented in the horizontal plane, while the second is oriented in the vertical plane. The ionized neutrals and incident ions were analyzed with identical ion spectrometers.

WINCS reproduced ion fluxes with point-by-point fidelity, providing error estimates for ion-drift, ion temperature, and densities fitting the data to the predicted Maxwellian fluxes. High precision in energy and angle was due to the clean ion-optics design of the spectrometer that relied on just two limiting apertures: the collimators first aperture plus the SDEA entrance aperture as the second collimator aperture. This design eliminated the need for electrostatic ion lenses, avoiding vignetting and distortion in the energy and angle distributions. The sharp focus of the SDEA made possible a trapezoidal energy bandpass rather than the typical triangular bandpass that ensured stable transmission to the SDEA detector. While the ion spectrometer performed successfully, the neutral side of WINCS failed.

The failure in the neutral measurements of WINCS was due to the neutral-to-ion conversion process. WINCS used an electron impact ion source of conventional design to measure energies and angles of the neutrals after ionization, but the size and strength of the space charge of the ionizing electrons distorted the trajectories to keep product ions from passing the SDEA aperture. The space charge effect is similar to the electron-electron repulsions that restrict electron emission in vacuum tubes. In laboratory ion sources, this issue is often ignored since the neutral gas velocity distribution prior to ionization is not of interest. The space-charge distortions impacting WINCS were analyzed showing that control of ionizing electron current and electron beam size was essential. A quantitative analysis shows that minimal distortions may be achieved with useful ion signal; for example, a 40μA electron beam confined to a thickness of 0.01cm along the path of the neutrals can yield an ion signal greater than 10^5 ions/sec at 400km altitude, where atomic oxygen density is on the order of 10^8/cm^3, and yet this signal strength allows for precise energy distributions with space-charge distortions below 0.013 eV for bulk velocity uncertainties about 10 m/s.

WIND has one primary instrument and a secondary instrument. The primary instrument described in this paper is WS, a combined neutral and ion spectrometer that uses the SDEA analyzer with the new aperture ion source AIS to obtain the neutral wind $\vec{W}$ and ion-drift $\vec{V}_I$ vectors with errors of about $\pm$10m/s with corresponding neutral and ion temperatures ($\pm 10^\circ$K) and densities ($\pm$10%). The secondary instrument is the gated electrostatic mass spectrometer GEMS [8], for composition of neutrals and ions with an expected mass resolution of 100 over the mass range 1 to 70AMU.

1. INTRODUCTION

In a gas like the thermosphere, the neutral number density n [#/cm^3] is the number of atoms and molecules per cm^3 that gives the mass density $\rho = \bar{m}n$ (e.g., in in g/cm^3) with $\bar{m}$ the mean molecular mass (in grams) averaged over all constituents [1]. A satellite with frontal area A moving with velocity $\vec{V}_{Sat}$ in a thermosphere with local wind $\vec{W}$ encounters $n \times V_{Ram} \times A$ particles per unit time in volume $V_{Ram} \times A$ swept by the satellite in unit time where $\vec{V}_{Ram} = \vec{V}_{Sat} + \vec{W}$. The sum of all particle collisions exert a drag force $F_D = 1/2\rho V^2 C_D A_r$, where A_r is the satellite area projected along vector $\vec{V}_{Ram}$ and C_D a dimensionless coefficient proportional to the fraction of momentum delivered per collision [9]. The drag force dissipates the satellite's total energy at the rate $P_D = F_D \times V_{Ram}$, reducing its altitude.

At any altitude and local time in the thermosphere from about 100 to 500km above the Earth the neutral density ρ shows a steady variation with longitude and altitude driven by solar Extreme Ultra-Violet (EUV or XUV) radiation. Absorbed at around 90 km altitude at local noon, this energy input leads to a temperature bulge around mid-afternoon that propagates upward into the entire thermosphere. The pressure gradients of this bulge drive neutral winds that transport mass, momentum and energy in interaction with neutrals and ions. Without external perturbations this steady state variation represents the tidal variations in density, temperature, and neutral winds with ion-drifts. Much is known about these variations and, beginning in the 1970's empirical models [10] used solar decimetric emission (F10.7) and other indices to predict the amplitudes of tidal variations. At the same time physics based models evolved solving the equations of continuity, momentum and energy transfer between neutrals and ions in the presence of the geomagnetic field [11, 12, 13, 14, 15]. Many of these models can introduce external perturbations like magnetic storms in response to solar flares, and also energy propagation from tropospheric storms or orographic features (e.g., the Andes mountain range with its vertically propagating waves [16, 18, 19, 20]; all showing significant variability to illustrate how waves from the lower atmosphere can drive space weather [21, 16]

One WIND instrument suite acting alone will provide some predictive power in combination with the tidal variations and other inputs like the solar F10.7cm flux or proxy for solar EUV radiation. For example, it is known that large zonal neutral winds can exist at high latitudes [2] and their longitudinal variation may be extended from the point where WIND measured (e.g. at the auroral oval) and some confirmation may be obtained in a subsequent orbital pass - such an event would lead to an increased force from the horizontal wind with effects that could accumulate for a net change in the orbit; however slight this deviation it may be sufficient to come near another satellite. It would be a complex problem to obtain likely collisions but WIND would provide the fundamental data required for such predictions.

Two WIND units would provide real estimates of gradients of all the parameters, and better yet with three and more. Ultimately, multiple WIND units will provide data on all thermosphere parameters at a sufficient number of points in the thermosphere to enable reliable predictions as desired over a Lat-Long-Altitude region. For satellites in VLEO and above it is possible, in principle, to predict neutral density enhancements at any point in the thermosphere where satellites fly.

It is important to begin with a small number of WIND units in orbit and increase gradually, testing the capability of the combined WIND-data assimilation schemes at every step of the way. Since WIND obtains in real time the signal to align its axis along the ram, the direction of minimum aerodynamic drag, every WIND unit has the capability of extending its orbital lifetime by minimizing drag.

The following sections describe the Wind Spectrometer WS in the WIND suite. It begins with the experimental method that uses the relation of measured particle fluxes to the desired parameters (wind, ion-drift, temperatures and densities), including sensitivity estimates to define instrument apertures and performance.

2. EXPERIMENTAL METHOD FOR NEUTRAL WIND, TEMPERATURE, DENSITY

The following sections describe the particle flux that must be measured highlighting its magnitude and energy-angle distributions, the approach to obtain the energy-angle distributions with consequent sensitivity snd detection issues, and finally a description of the Wind Spectrometer that consists of a collimator, ion source AIS, and energy analyzer SDEA.

2.1 Particle Flux

Earth's thermosphere and ionosphere being in thermodynamic equilibrium, the neutrals and ions have Maxwellian velocity distributions[1]. A spectrometer measuring the energy-angle distributions impacting a satellite moving with velocity $\vec{V}_{Sat}$ through a wind $\vec{W}$ will detect fluxes of neutrals and ions incident centered around the ram velocity vector $\vec{V}_{Ram} = \vec{V}_{Sat} + \vec{W}$. Since the neutral gas is in equilibrium with the ion gas (the ionosphere), the fluxes of neutrals and ions are maximum along $\vec{V}_{Ram}$ whose direction is easily identified in the satellite frame of reference and thereby in the spectrometer. Selecting the x-direction along the $\vec{V}_{Ram}$ and with particle velocity $\vec{v} = (v_x, v_y, v_z)$, the Maxwellian

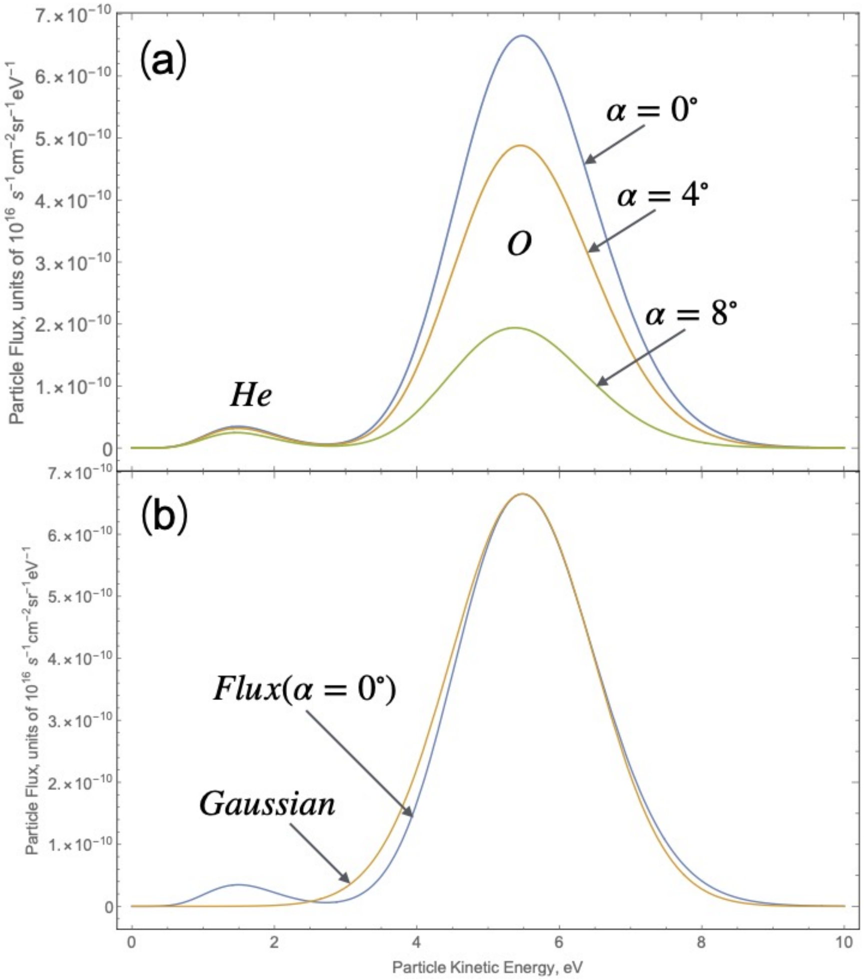

Fig. 1: (a) Energy variation of expected flux at 400 km in a 1000°K thermosphere with atomic oxygen O and helium He for 3 angles. (b) Flux function shows its skewness compared to the symmetric Gaussian peaking at the same energy.

velocity distribution measured in the satellite is a drifting Maxwellian with drift velocity $\vec{V}_{Ram}$ and may be measured onboard a satellite as

$$f_i(v_x, v_y, v_z) = A_i e^{-((v_x - V_{Ram})^2 + v_y^2 + v_z^2)/a_i^2} \ , \tag{1}$$

with $A_i = n_i/(\pi a_i^2)^{3/2}$, $a_i = \sqrt{2k_B T/m_i}$, k_B Boltzmann's constant, and m_i the mass of the i^{th} species. With present resources it is most convenient to measure kinetic energy $K(= 1/2m_i v^2)$ close to $\vec{V}_{Ram}$ within two angles (θ, τ) measured from $\vec{V}_{Ram}$ instead of three velocities (v_x, v_y, v_z). The flux as a function of (K, θ, τ) is obtained with a transformation from (v_x, v_y, v_z) to (K, θ, τ) with v_x pointing along $\vec{V}_{Ram}$[17, 6]. The particle flux for the i^{th} species of mass m_i is

$$F_i(K, \theta, \tau) = \frac{2n_i \sec^2\theta \sec^2\tau \cos^4\alpha(\theta, \tau)}{(2\pi k_B T)^{3/2} {m_i}^{1/2}} \times K e^{-(K - 2\sqrt{(KK_{iT}}\cos\alpha(\theta,\tau)) + K_{iT})/k_B T}, \tag{2}$$

with flux units [$\text{cm}^{-2}\text{s}^{-1}\text{sr}^{-1}\text{eV}^{-1}$], $K_{iT} = 1/2m_i V_{Ram}^2$, and $\alpha(\theta, \tau)$ the angle between $\vec{V}_{Ram}$ and $\vec{v}$, satisfying $\cos\alpha(\theta, \tau) = 1/\sqrt{1 + \tan^2\theta + \tan^2\tau}$. The flux peaks at specific values of K depending on K_{iT} and $\alpha(\theta, \tau)$, Fig.1a showing the energy distributions in a thermosphere with helium He and atomic oxygen O at three angles of incidence $\alpha = 0°, 4°, 8°$. The flux maximum at $\alpha = 0°$ locates the direction of $\vec{V}_{Ram}$ in the satellite frame. Fig.1b illustrates how closely the spectrometer must follow the true skewed shape of the energy distribution if it is to obtain parameter values with desired uncertainties - the closeness to a fictitious symmetric Gaussian peaking at the same energy illustrates how precise the data must be. That is, data points must reproduce this skewed shape for precise determinations of the parameters K_{iT} and T as demonstrated in orbit to high precision with the energy analyzer SDEA in WINCS[6] that also gave evidence that Maxwellian fluxes and consequently thermodynamic equilibrium persist up to 550km.

2.2 Spectrometer Function

Fig. 1 suggests that a full measurement of the energy and angle distributions of the atomic oxygen (AO) flux near the angle of maximum flux $\alpha = 0°$ may be sufficient to obtain the wind and ion-drift vectors and the remaining 4 parameters. A spectrometer field of view of about 16° full-angle suffices to check that the spectrometer is pointing along the maximum to also estimate the crosswind component in the plane of 16° field of view. It has been shown in WINCS [6] that the temperature may be obtained from the energy distribution to use in estimating the full angular width of the flux in the number density calculation. To estimate required kinetic energy precision ΔK in terms of required wind velocity uncertainty Δv, we note that $\Delta K/K = 2(\Delta v/v)$. With the present goal of $\Delta v = \pm 10$m/s uncertainty in neutral wind investigations, a neutral AO flux incident with $V_{Ram} \simeq 8,000$m/s has total kinetic energy $K_{iT} = K_{OT} \simeq 5$eV requiring a $\Delta K = 2(\Delta v/v) \times K = 0.013eV$. In the rest of the paper $\Delta K = 0.013$eV is taken as the maximum permissible distortion in the electron impact ionization source (EIIS) with AO taken as the sole constituent in the thermosphere.

With those considerations, our design uses a rectangular field of view of $\Delta\alpha \times \Delta\beta = 2° \times 16°$ defined by an entrance slot .64cm×.1cm and s_u a 0.1cm diameter slit located 6cm beneath the slot; the $\Delta\alpha = 2°$ value is required to obtain energy resolution $\Delta K/K$ of 0.1 or better with the energy analyzer. Figure 2 illustrates with exaggerated angles that the field of view may be considered as a set of 8 adjacent angular pixels $2° \times 2°$, each one passing s_u, two such pixels shown[4]. The rectangular slot and aperture of diameter s_u are separated by a distance that gives $\Delta\alpha \times \Delta\beta = 2° \times 16°$ and no other aperture in between or after restricts the particles on their way to the energy analyzer. Aperture s_u is the entrance aperture of the energy analyzer, the SDEA Chamber, and neutrals are ionized a short distance above s_u. The energy analyzer accommodates all 8 pixels deflecting the ions according to their energies in the α-plane while they move undeflected in the β-plane. As described below, the SDEA detector has a 2-dimensional array displaying the energy and angle distributions. In WIND, the distributions will be analyzed onboard for both neutrals and ions to yield $(\vec{W}, T, n_O, n_{N_2})$, atomic oxygen O and N_2 expected as the major constituents above 200km altitude. Similarly with $(\vec{V}_{ID}, T, n_{O^+})$ for the ions. Of course no ionization is required for the ambient ion data set.

2.3 Detection and Sensitivity

Detection of neutrals requires neutral-to-ion conversion. WIND uses an electron impact ion source of the AIS geometry to offer minimal distortion of the energies and angles of its ion products - AIS overcomes the problem encountered in WINCS in which neutral measurements were not possible because of ion source distortions. In WIND, neutral-to-ion conversion occurs in the AIS, care taken to deflect the incident ions during the neutral measurement. Detection of ions is direct as they pass through an inactive AIS with its electrodes all at chassis ground. This way incident ions and neutrals (their ion products) are analyzed identically and registered at the energy analyzer position sensitive detector. WIND uses a Micro-Channel-Plate MCP electron multiplier with multiple anodes that provide the energy and the angle.

Figure 2 shows the function of the collimator on the particle flux. The particle flux contains neutrals and ions and enter the first slit s_i of the collimator, the solid angle $\Delta\Omega_i$ representing the cone within which all atoms of the i^{th} species move; other neutrals and ions will have their own $\Delta\Omega$'s each calculable from the temperature obtained in the energy distribution. Of these, only those within the smaller solid angle $\Delta\omega$ pass the second collimator slit s_u. The fraction of the incident flux $F_i(K,\theta,\tau)$ that passes s_u is $\Delta\omega/\Delta\Omega_i$ and may be called the sensed flux $F_{S-i} = F_i(K,\theta,\tau) \times (\Delta\omega/\Delta\Omega_i)$. Now, eq. 2 shows that $F_i(K,\theta,\tau)$ depends explicitly on n_i and may be written as $F_i(K,\theta,\tau) = n_i \times f_i(K,\theta,\tau)$ to give

$$F_{S-i} = n_i \times (\Delta\omega/\Delta\Omega_i) \times f_i(K,\theta,\tau) \rightarrow n_{S-i} = n_i \times (\Delta\omega/\Delta\Omega_i), \tag{3}$$

n_{S-i} being the neutral density in the ionization region of the ion source. For Atomic Oxygen $\Delta\Omega_O = 2\pi(1-\cos\theta_O) =$ .054sr, $\theta_O \simeq 7.5°$ being the half-angle of the cone containing most AO atoms in the incident flux ($\theta_O = \tan^{-1}\sqrt{2k_BT/m_O}/V_{Ram}$). $\Delta\omega = 2\pi(1-\cos(1°)) = 9.6 \times 10^{-4}$sr. Therefore, $(\Delta\omega/\Delta\Omega_O) = 0.018$, making $n_S = 0.018 n_O$. With this estimate it is now possible to estimate the ion signal that enters s_u to be analyzed in energy and angle.

[4]Strictly speaking the pixels should be square to be considered adjacent but little is lost in the estimates of transmitted flux that matter for our design.

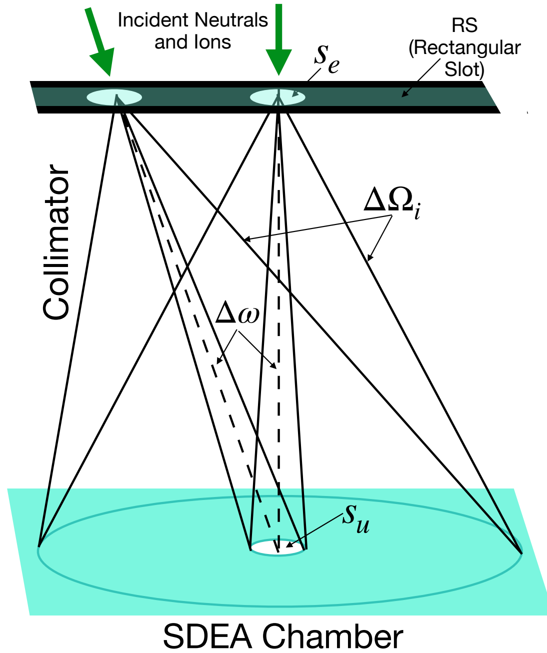

Fig. 2: Flux of neutrals and ions entering rectangular slot RS treated as 8 adjacent slits of diameter s_e (only two shown with angles exaggerated for illustration); each pixel with solid angle $\Delta\omega$ divergence out of $\Delta\Omega_i$ for full particle flux of the i^{th} species. Each of the 8 divergent cones pass through exit slit of diameter s_u. The fraction of the flux passing to the SDEA chamber is $(\Delta\omega/\Delta\Omega_O)$. The β-plane in the plane of the paper is perpendicular to the α-plane.

2.4 The Electron Impact Ion Source

In the ion source, electrons ionize a fraction of the neutrals in the target gas, the ions in this fraction known as the product ions. These product ions are pulled within the ionization region in one direction or another depending on the number of electrons contained in those directions. The more time an ion spends inside the electron cloud the more it departs from its original velocity - an effect that by itself changes the energy and angle distributions of the product ions and led to the failure of the neutral measurements in WINCS.

At the beginning of the WIND project this problem was analyzed leading to the obvious conclusion that a very shallow electron beam may reduce the changes in the product ion trajectories to tolerable levels - but the question was what thickness must the electron beam have and what small electron current was tolerable for a given thickness, and furthermore, would the reduced electron current yield a useful ion signal. A quantitative estimate of the effect was necessary and based on that analysis[7] we adopt a 0.1mm thick electron beam with 40μA current to guarantee an energy distortion less than our desired 0.013eV maximum permissible distortion. The electron beam is kept very close to the aperture s_u which is the smaller of the two apertures of the AIS as shown in Figure 3 discussed further below.

Onboard a satellite as in the laboratory, an electron impact ion source yields ion current I_I from a target gas of number density n [#/cm^3] with ionizing electron current I_e passing through the target gas. I_i may be obtained as initial electron current I_{e0} attenuates to $I_e = I_{e0}e^{-\sigma_I nx}$ if every electron lost from I_e produces one ion. Since $\sigma_I nx << 1$ the ion yield is accurately given by

$$I_I = \Delta I_e = I_{e0}(1 - e^{-\sigma_I nx}) = I_e \sigma_I nx \tag{4}$$

where the electron impact ionization cross section $\sigma_I \approx 2 \times 10^{-16}$cm^2, $x =$ the ionization path length approximately the same as the aperture diameter s_u, and $n = n_S = .018n_O$ in our case. The atomic oxygen density n_O at 400km is about 10^8/cm^3 giving $n_S \simeq 2 \times 10^6/\text{cm}^3$. The ion signal, from eq.4 is about 10^4ions/sec., sufficient to yield valid determinations of the thermosphere parameters to be telemetered to the ground for further analysis combining the 10 parameters with auxiliary data (e.g., from ground-based facilities, sounding rockets, and other satellites) for effective prediction of neutral density.

2.5 The Wind Spectrometer WS

The left panel of Figure 3 illustrates in a side view the three parts of the wind spectrometer WS. Atomic oxygen being a major constituent, its flux Φ_O is shown entering the instrument at the top. Particles enter the COLLIMATOR (between plates P1 and P2), and a small fraction of those enter the aperture ion source AIS for neutral-to-ion conversion, its top plate labeled P3 and ions exiting at aperture s_u on P3; the ion products enter the energy analyzer at aperture s_u on plate P3 to be energy analyzed in the SDEA between P3 and P4. The right panel shows an assembly of the WS with the mechanical drawings of its parts.

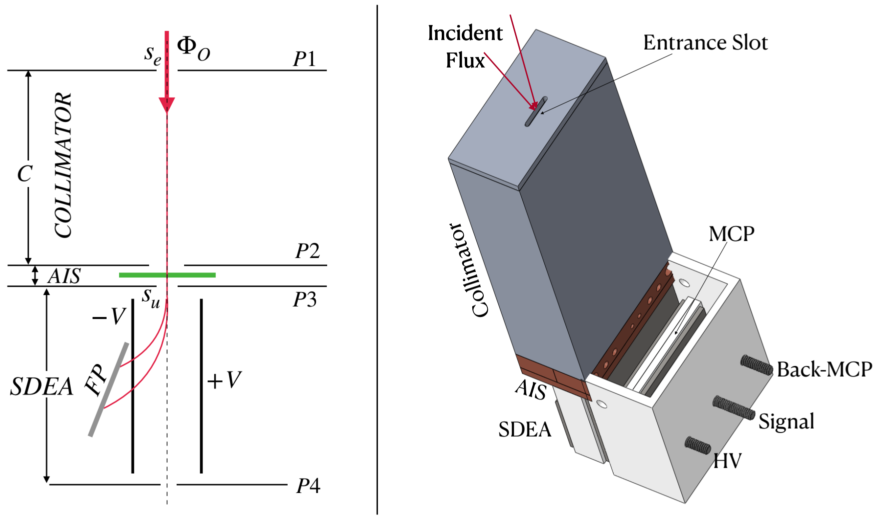

Fig. 3: Left panel: schematic layout of the three components of WS: the COLLIMATOR, the ion source AIS, and the energy analyzer SDEA. The right panel shows as 3-dimensional assembly of the mechanical drawings of the WS. The height of the collimator is 2.2cm and provides a measure of the scale of the WIND WS instrument in the 3-D drawing.

As in Fig. 2 the COLLIMATOR restricts the range of angles of particles passing s_u to within the narrow solid angle $\Delta\omega$ as required by the energy analyzer; in our case about 1.8% of the flux passes s_u. Collimation is achieved with two limiting apertures of diameters s_e and s_u separated by distance C - in our case $s_e = s_u$; its cone of acceptance $\Delta\omega$ being set by the ratio s_e/C. Another function of the COLLIMATOR is to isolate the neutral flux from the ambient ion flux in an ion-trap not shown in the Figure. WS has two modes of operation to measure neutrals only in Neutrals-Mode or ions only in Ions-Mode as commanded by the WS electronics. In the Neutrals-Mode the ion-trap inside the COLLIMATOR removes the ions that would enter WS at s_e on P1 and contaminate the neutral signal. The ion-trap consists of an ion deflector with several baffles to absorb ambient ions on the internal surfaces of the COLLIMATOR - not shown in Figure 3.

The Aperture Ion Source AIS consists of two plates, P2 and P3 with neutral-to-ion conversion carried out by a shallow electron beam represented by the green bar between P2 and P3 that are separated by 2mm. The thickness of the electron beam is 0.1mm with most of the neutral-to-ion conversion occurring inside and about 1mm above AIS aperture s_u of diameter $s_u = .076$cm. Ion signal expected from the AIS is about 10^4 ions/sec at 400km altitude, increasing at lower altitudes and decreasing higher up.

On SDEA, the left panel of Figure 3 shows that SDEA deflects ions with the electric field set up between its deflector plates by voltages $+V$ and $-V$. SDEA focuses ions that pass its entrance aperture s_u at different energies simultaneously, illustrated by the two red curved trajectories. Ions converge at the focal plane FP with magnification $m \simeq .01$ - that is, ions filling diameter $s_u = 1$mm at the SDEA entrance are focused to a .01mm spot. This makes it possible to detect and register simultaneously a kinetic energy range from 0 to 12 eV to include both atomic oxygen O of mass 16amu and molecular nitrogen N_2 with mass 32amu, O and N_2 being the dominant species to be detected in Low-Earth-orbit in the thermosphere. The simultaneous energy range is enabled by our new rectangular MCP assembly with sensitive area 10mm$\times$8mm manufactured by Photonis, Sturbridge, MA, USA. It is shown in the right panel Fig.3 with its connections for high voltage HV (1800 to 2400 volts DC) and a single anode Signal lead to be used in our

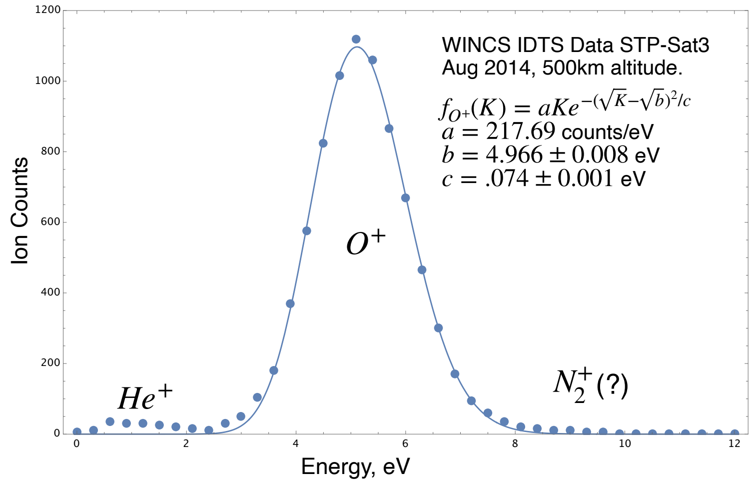

Fig. 4: IDTS energy distribution obtained at $\alpha = 0^\circ$ with fitting function and parameters shown in the legend. The fitting function $f_O(K)$ was obtained from Eq.2 for $\alpha = 0$ and atomic oxygen ion O^+ with parameters a for amplitude in counts/eV, $b = K_{O^+}$ in eV, and $c = k_B T$ in eV, with $k_B = 8.617 \times 10^{-5}$ eV/K. Details in text.

initial laboratory tests. The MCP is a pair of plates mounted in Chevron form providing a gain of about 10^7 electrons per ion detected.

The anode at the back of the MCP detector gives the ion energy along one direction and the angular distribution in the $\perp$ direction. The angular distribution measures the deviation from $\vec{V}_{Ram}$ and may be used by the spacecraft to point into the ram continuously. In addition this information gives the neutral wind component along the plane of the entrance slot shown in the right panel of Figure 3

Finally, the aperture on P4 allows venting and laboratory alignment, the venting helping to reduce pressure buildup inside the instrument - important at low altitudes since the MCP may be sensitive to pressures exceeding 10^{-6} Torr.

The expected WS neutral energy distribution is similar to the ion spectrum obtained with the WINCS Ion-Drift Temperature Spectrometer IDTS[6]; the example in Figure 4 showed an O^+ peak near $K = 5$ eV and a much smaller He^+ peak around 1.2 eV but no N_2^+ peak. The closeness of the data points (blue dots) to the continuous curve of the flux function of eq.2 is a feature of the SDEA due to the clean ion-optic design of SDEA that uses only two limiting apertures as in Fig.3. The fitting function for the O^+ peak is given and was taken directly from eq.2 for $\alpha = 0$; it was $f_{O^+}(K) = aKexp(-(\sqrt{K} - \sqrt{b})^2/c)$ with kinetic energy K, and parameters a proportional to number density n_{O^+}, $b = K_{O^+}$, and $c = k_B T$. The peak amplitude $aK = 217.69 \times 4.966 = 1081$cts from which the number density may be obtained; $b = K_{O^+} = 4.966 \pm 0.008$eV, the 0.008 eV error corresponding to $\pm$6m/s in the velocity (wind or ion-drift) of the ions or neutrals, respectively; $ck_B T = .074 \pm 0.001$eV corresponds to $T = 859 \pm 12$Kelvin. The same ion-optic design is followed in WIND. The example shown was taken at high altitude above 500 km, and that may explain the absence of the N_2^+ peak.

3. SUMMARY AND CONCLUSIONS

Prediction of the position and time of neutral density enhancements in the thermosphere/ionosphere system are required for satellite collision avoidance. The physics of the thermosphere/ionosphere involves transport of mass, momentum, and energy within it, its properties identified as 10 parameters that are tightly coupled in their spatial evolution in time. Hence, prediction of density requires knowledge of the other 9 parameters.

Thermal equilibrium in the thermosphere/ionosphere makes it possible to infer the neutral wind, temperature and density and same for the ions from simultaneous in-situ measurements of kinetic energy and angle distributions of the neutral and ion fluxes incident on an orbiting spectrometer. A new charged-particle spectrometer WS has been designed to accomplish this and is currently under construction. The instrument suite WIND has been designed, its principal instrument being the wind spectrometer WS to be tested after assembly; a secondary instrument is a mass spectrometer to provide detailed ion and neutral composition. Multiple WIND units will orbit in multiple orbits to obtain and telemeter the 10 parameters to ground stations with a maximum cadence of 1 set of the 10 parameters per second. The parameters consist of the three bulk velocity components and temperature with densities for neutrals and ions and may be listed as $(u, v, w, T, \rho), (u_I, v,_I w_I, T_I, \rho_I)$.

WS has energy analyzer heritage from the WINCS instrument suite flown in several satellites. While the WINCS ion spectrometer demonstrated the experimental method used in WS and established that indeed thermodynamic equilibrium fluxes can be measured up to an altitude of 550km, its neutral spectrometer failed. Investigation of that failure led to the design of the AIS ion source for WS.

Thus, the two obstacles to the measurements of the 10 parameters were overcome with AIS and the SDEA analyzer inherited from WINCS; the new ion source AIS is designed to yield sufficient signal to measure the neutral energy-angle distributions with minimal distortion, the distortion being small enough to allow an error of $\pm$10m/s in the wind components, and a new version of the energy analyzer SDEA developed for enhanced sensitivity with its 2-dimensional focal plane that covers the entire energy range and angular field of view instantaneously.

While the methodology for WIND has been demonstrated with the WINCS ion spectrometer, the neutral measurements need to be demonstrated and this will be WIND's role. How many WIND units will be required operating simultaneously to obtain reliable predictions is at this point an open question, and even with a sufficiently broad coverage over the thermosphere there may be implementation issues in the data assimilation process with NOAA's computers. Many such implementation issues are more easily addressed with a small number of WIND units orbiting and collecting data. Therefore it is prudent to begin with perhaps one or two WIND units, taking advantage of ground-based observations of possible perturbation events (i.e., waves propagating from tropospheric events below, solar events, and other sources). Use of known symmetries (auroral ovals, equatorial F-region dynamo,...) abound to help make the most of observations with a single unit with predictions tested in subsequent passes of the satellite-borne WIND units. As experience evolves and new lessons are learned it will soon become apparent how large a constellation of orbiting WIND units may be required to obtain predictions of neutral density enhancements with some estimable degree of confidence.

REFERENCES

[1] P. M. Banks and G. Kockarts, *Aeronomy.* (Academic Press, New York, 1973).

[2] N. W. Spencer, L.E. Wharton, G.R. Carignan, and J.C. Maurer, Thermospheric zonal winds, vertical motions and temperatures as measured from Dynamics Explorer, Geophys. Res. Lett., 9, 953-956, 1982.

[3] F. A. Herrero, H. G. Mayr, N. W. Spencer, .A. E. Hedin and B. G. Fejer, Interaction of zonal winds with the equatorial midnight pressure bulge in the Earth's thermosphere: empirical check of momentum balance, Geophys. Res. Lett., 12, 1985.

[4] A. C. Nicholas, F. A. Herrero, A. W. Stephan, T. Finne, WINCS on-orbit performance results, Proceedings of the SPIE, Volume 9604, id. 960404 15 pp. (2015). DOI 10.1117/12.2188403, 2015.

[5] A. C. Nicholas, F. A. Herrero, T. Finne, D. Aalami, and H. H. Jones, Preliminary results from the WINCS sensor on the NASA Green Propellant Infusion Mission, AGU paper SA33B-3144, 11 December 2019.

[6] F. A. Herrero, A. C. Nicholas, T. Finne, H. H. Jones, and D. Aalami, The small-deflection energy analyzer (SDEA): Enabling multi-point investigations in the thermosphereionosphere, Rev. Sci. Instruments, 91, 095105 (2020); https://doi.org/10.1063/5.0001903.

[7] F. A. Herrero, The Electron impact ion source: distortion of its product ion velocities, preprint SSRC, submitted to Rev. Sci. Instruments, June 2025.

[8] F. A. Herrero, H. H. Jones, and J. G. Lee, The Gated Electrostatic Mass Spectrometer (GEMS): Definition and Preliminary Results, J. American Soc. Mass Spectrometry, 19, 1384-1394 (2008).

[9] F. A. Herrero, The Lateral surface drag coefficient of cylindrical spacecraft in a rarefied finite temperature atmosphere," AIAA Journal, 23, 862, 1985.

[10] A. E. Hedin, J. E. Salah, J. V. Evans, C. A. Reber, G. P. Newton, N. W. Spencer, D. C. Kayser, D. Alcayd, P. Bauer, L. Cogger, J. P. McClure, A global thermospheric model based on mass spectrometer and incoherent scatter data, MSIS 1, N2 density and temperature, J. Geophys. Res., 82, 21392147, 1977.

[11] R. E. Dickinson, E. C. Ridley and R. G. Roble, A three-dimensional general circulation model of the thermosphere, J. Geophys. Res., 86, 1499-1512, 1981.

[12] R. E. Dickinson, Ridley E, Roble R. Thermospheric general circulation with coupled dynamics and composition. Journal of the Atmospheric Sciences, 41(2), 205219, 1984.

[13] A. D. Richmond, Ridley EC, Roble RG. A thermosphere/ionosphere general circulation model with coupled electrodynamics. Geophysical Research Letters, 19(6):601604, 1992. doi: 10.1029/92GL00401.

[14] R. Roble, Ridley E, Richmond A. A coupled thermosphere / ionosphere general circulation model. Geophys Res Letters,15:13251328, 1988.

[15] T. W. Fang, Richmond A, Liu J, Maute A, Lin C, Chen C, Harper B. Model simulation of the equatorial electrojet in the Peruvian and Philippine sectors. J Atmos Sol-Terr Phys. 2008;70(17):22032211. doi: 10.1016/j.jastp.2008.04.021.

[16] T. Fuller-Rowell, E. Yizengaw, P. H. Doherty, S. Basu, *Ionospheric Space Weather Longitude Dependence and Lower Atmosphere Forcing* American Geophysical Union, issuing body. Hoboken, New Jersey: Wiley, 2017.

[17] F. A. Herrero, A Gas Kinetic Method for Investigations of the Ionospheric Plasma and the Thermosphere, Radiation Effects and Defects in Solids: Incorporating Plasma Science and Plasma Technology, 168, 833-846, 2013.

[18] J. W. Meriwether, J. L. Mirick, M. A. Biondi, F. A. Herrero, and C. G. Fesen, Evidence for orographic wave heating in the equato rial thermosphere at solar maximum, Geophys. Res. Letters, 23, 2177-218, 1996.

[19] G. Malhotra, T. FullerRowell, T-W. Fang, A. M. Kubaryk, MediumScale Thermospheric Gravity waves in the highresolution Whole Atmosphere Model: Seasonal, local Time, and longitudinal variations, Journal of Geophysical Research: Atmospheres, 130, xxx-xxx, 2024.

[20] T-W. Fang, R. Akmaev, T. Fuller-Rowell, F. Wu, N. Maruyama, G. Millward., Longitudinal and day-to-day variability in the ionosphere from lower atmosphere tidal forcing. Geophysical Research Letters, 40(11), 25232528, 2013. https://doi.org/10.1002/grl.50550

[21] T. Fuller-Rowell, Wu, F., Akmaev, R., Fang, T.-W., Araujo-Pradere, E. (2010). A whole atmosphere model simulation of the impact of a sudden stratospheric warming on thermosphere dynamics and electrodynamics. Journal of Geophysical Research, 115(A10). https://doi.org/10.1029/2010JA015524